Defects and Spacelike Properties of Delayed Dynamical Systems

G. Giacomelli,[1,2] R. Meucci,[1] A. Politi,[1,3] and F. T. Arecchi[1,4]
[1]*Istituto Nazionale di Ottica, 50125 Firenze, Italy*
[2]*ITIS "Tullio Buzzi," Prato, Italy*
[3]*INFN, Sezione di Firenze, Firenze, Italy*
[4]*Dipartimento di Fisica, Universitá di Firenze, Firenze, Italy*
(Received 11 January 1994)

In a laser with delayed feedback operating in an oscillatory regime, phase defects appear for delays longer than the oscillation period. These defects are visualized by rearranging the data in a two-dimensional representation. Two distinct disordered phases are observed, one of weak turbulence characterized by phase fluctuations, and one of highly developed turbulence characterized by a constant density of defects. The transition between the two regimes is analyzed by studying the dependence of the defect lifetime on the delay. The experimental findings are modeled via a generalized Landau equation which includes a delayed coupling.

PACS numbers: 42.50.Lc, 05.45.+b

Thus far, most of the interest in delayed dynamical systems (DDS) has been restricted to models of the type

$$\dot{x} = -\gamma x + F(x(t-\tau)), \quad (1)$$

where F is a nonlinear function and τ the delay time. For zero delay, Eq. (1) describes the evolution of a single degree of freedom. Both the Mackey-Glass equation [1], modeling the formation of blood cells, and the Ikeda equation [2], accounting for the evolution of a nonlinear optical resonator, belong to this class. The fact that a DDS has an infinite-dimensional phase space suggests that it may be assimilated to a spatially extended system (SES). Indeed, a close analogy between the two classes of systems is discovered by formally decomposing the time variable t of a DDS into a continuous spacelike variable σ ($0 \leq \sigma \leq \tau$) and a discrete timelike variable n [3],

$$t \equiv \sigma + n\tau. \quad (2)$$

Accordingly, the long-range coupling associated with the delayed feedback can be seen as a local interaction from one to the next delay unit. As a consequence, the signal $x(t)$ arising from a DDS can be rearranged as a 2D pattern of a 1D SES of length $L = \tau$ on a discrete-time lattice. The scaling behaviors of the chaotic indicators in the long-delay limit [4–7] are translated into equivalent properties of extended systems in the thermodynamic limit $L \to \infty$. For instance, while the Lyapunov spectrum of a SES is size independent, in the case of a DDS it scales as $1/\tau$ [4]; however, by adopting the time unit defined in Eq. (2), a size independency is recovered also for the DDS [8].

In the case of a laser with delayed feedback, even for zero delay the dynamics implies 3 degrees of freedom [9]; thus, for suitable parameter values, the system undergoes regular or chaotic oscillations. In this Letter, we report evidence of phase defects in this system, for delays long with respect to the oscillating period. The defect localization and their statistical characterization are made possible by the space-time representation introduced above [3]. Even though the detailed three-equation model [9] of the laser with feedback reproduces these findings, we will show that a simple, Landau-type equation is sufficient to grasp the crucial aspects of this phenomenon.

The experimental setup has already been described in Ref. [9]. It consists of a single-mode CO_2 laser with a delayed feedback on the losses, realized via an intracavity electro-optic modulator, driven by a signal proportional to the output intensity, delayed and amplified by a high voltage amplifier. The bias B of the amplifier is the control parameter of the system. The delay line was specifically designed using fast (2 MHz) and accurate (12 bits) A/D and D/A (analog-to-digital) converters with a digital control, allowing us to vary τ from 0.5 μs to 131 ms. The signal acquisitions were performed using a

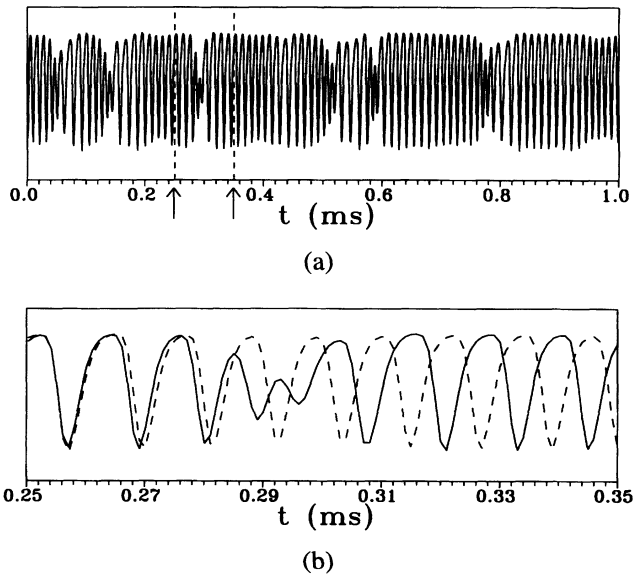

FIG. 1. (a) Intensity signal within a delay unit (τ = 1 ms, B = 159 V); (b) expanded view of the signal between the arrows exhibiting a phase jump (solid line) and reference signal (dashed line) translated from a regular region without noticeable intensity variations.

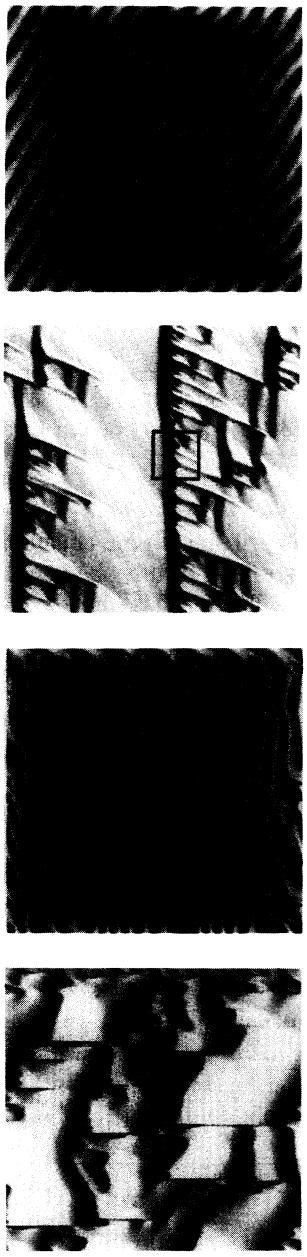

FIG. 2. Space (horizontal)-time (vertical) plots of the experimental signal for $B = 160$ V and $\tau = 0.8$ ms [(a), (b) and of the solutions of (3)] for $\mu = 0.5$, $\beta = 2$, and $\tau = 50$ [(c), (d)]. Time increases downward. (a) is a plot of the actual experimental signal, while (b) is the envelope amplitude after demodulation of the carrier (800 delay units are reported). The pattern in (a) corresponds to the boxed region in (b). The pattern reported in (c) is the 2D representation of $\mathrm{Re}\{x(t)e^{i\omega n}\}$, where $\omega = 1.2$ is a phase shift introduced to better reveal the oscillations of the signal (500 delay units are reported). The corresponding envelope amplitude is shown in (d). In cases (b) to (d), the horizontal width has been suitably set to a value slightly larger than τ to eliminate the systematic drift of the main structures. The defects appear as fringe dislocations in a quasisinusoidal pattern [(a), (c)] or as black regions in the envelope representation [(b), (d)].

12 bits A/D converter (LeCroy 6810), paced by a 1 MHz clock synchronized with that of the delay line.

In the case of an instantaneous feedback, the laser undergoes a direct Hopf transition beyond a critical bias, from a stationary to an oscillating regime. Further beyond, a Q-switched regime is found, characterized by an increasing time separation between the spikes, until the laser switches off. A qualitatively similar scenario is found in the presence of a delay longer than the Hopf period; however, in this latter case, the oscillations are irregular.

The intensity signal is reported in Fig. 1(a) for $\tau = 1$ ms and $B = 159$ V, close to the Hopf bifurcation value $B_c = 138$ V. Trains of regular oscillations are interrupted by localized events, where the phase of the signal suddenly changes and the amplitude markedly decreases as shown in Fig. 1(b) where the phase jump is demonstrated by the superposition with a more regular portion of the signal (dashed line). This behavior is reminiscent of space-time defects in 1D extended systems; see, e.g., Ref. [10]. The space-time representations of Fig. 2 clarify this analogy. The "spatial" length L has been set to a value slightly larger than τ in order to eliminate a slow systematic drift exhibited by the regions of small amplitude oscillations and thus have the black regions approximately vertical. Besides the vertical backbone, the dark regions exhibit also lateral asymmetrical branches whose fluctuating length is associated with the long time decay (several τ units) of the autocorrelation function discussed in Ref. [3].

Along the dark regions we find points where the circulation of the 2D gradient of the phase yields an integer multiple of 2π [Fig. 2(a)]. These dislocations correspond to phase singularities which, as in a 1D SES [11], can be understood only by analyzing the 2D pattern resulting from the space-time representation: In fact, there are no topological constraints for phase and amplitude in a 1D space. The above analysis provides a meaningful interpretation of the π phase jumps often recognized in the time plots [see, for instance, Fig. 1(b)]. In such cases, the 2D representation shows perturbed regions where the extra fringe develops over many fringes (as in Fig. 2).

In fact, the discrete nature of the time axis (n) prevents an accurate identification of a defect, and this casts doubts upon the very existence of singular points characterized by zero amplitude. However, since the defect cores are spread over many delay units, it appears possible to extend the two-dimensional phase function $\phi(\sigma, n)$ to noninteger n values and, hence, to position a defect. For the moment we adopt an even more heuristic point of view and locate a defect where the oscillation amplitude is smaller than some preassigned threshold.

By increasing the bias B above the Hopf bifurcation, two different regimes are encountered: *defect-mediated turbulence* (*DT*), where defectlike structures are observed over all times, and *phase turbulence* (*PT*), where, after

a short transient, only limited amplitude fluctuations accompanied by phase fluctuations are detected. To characterize the two regimes we investigate the defect evolution. As the loop is closed, an electronic switch inserted in the feedback loop provides a trigger signal to the acquisition electronics. We evaluate the transient lifetime T of the defects, by performing measurements at fixed τ for several B values. Each data point is averaged over several runs. The results, reported in Fig. 3(a), clearly show the transition between distinct regimes. The large error bar close to the transition point is an indication of the critical enhancement of the fluctuations. Notice that the largest measured lifetimes are thousands of delay units.

The next relevant question concerns the persistence of the two regimes in the thermodynamic limit $\tau \to \infty$. The dependence of T on τ, reported in Fig. 3(b), for two parameter values lying on opposite sides of the transition, answers the question. An exponential growth is found for $B = 155$ V, while the results for $B = 175$ V are fitted with a power law $T \simeq \tau^{\alpha}$ with $\alpha = 0.7$. Within the statistical accuracy, the value of the exponent is compatible with 0.5, a value that we would expect from a diffusive motion of the defectlike structures.

Finally, we directly test the validity of the assumption that the low-amplitude regions are associated with defects.

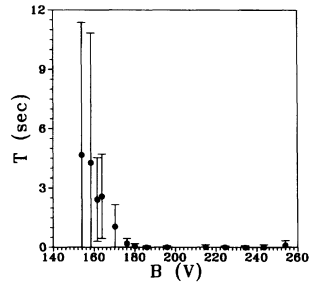

(a)

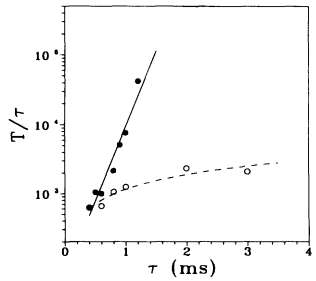

(b)

FIG. 3. (a) Average transient lifetime T of defects for $\tau = 1$ ms displaying a transition from an asymptotically ordered (high B) to a disordered (low B) regime; (b) scaling of T with the delay τ for $B = 155$ V (full circles) and $B = 175$ V(open circles). The solid line is an exponential fit of the data; the dashed line is a power law with an exponent 0.7.

By suitably filtering the signal, we demodulate it, so that we can compute the integrated probability distribution $P(A)$ that the envelope be smaller than A. The results for two different B values are reported in Fig. 4(a). A striking difference is again found in the two regimes: For $B = 200$ V the support of the distribution is limited to a narrow interval, whereas arbitrarily small values of A have finite probability in the DT regime ($B = 160$ V). Indeed, the small-A behavior of the histogram turns out to be a power law, $P(A) \simeq A^{\nu}$ with the exponent $\nu \simeq 2.3$.

A theoretical analysis of our experiment can be carried along guidelines similar to those adopted for a SES. Recent numerical investigations of a 1D SES [11] are based on the complex Ginzburg-Landau equation (CGL), which describes a nonlinear extended system in the vicinity of a Hopf bifurcation. Such an equation reproduces many of the phenomena also observed in our laser system. For instance, the CGL generates small amplitude localized structures which play a relevant role in triggering a turbulent behavior [12]. In our case, in order to account for the peculiar properties of a DDS which give rise to a phenomenology not completely equivalent to that of a SES [8], we introduce the following delayed equation:

$$\dot{x} = \mu x - (1 + i\beta)|x|^2 x + (1 + i\varepsilon)x(t - \tau), \quad (3)$$

where x is a complex variable and μ, β, and ε are real parameters. This equation is a delayed version of the complex Landau equation. It contains the same local interaction term, accounting for the observed Hopf bifurcation. At variance with the CGL, Eq. (3) includes

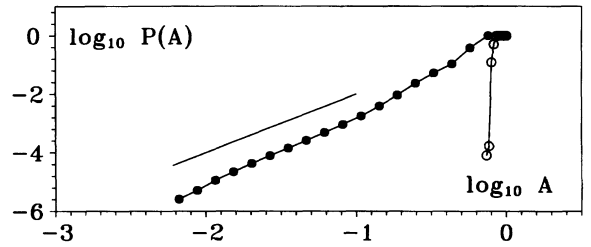

(a)

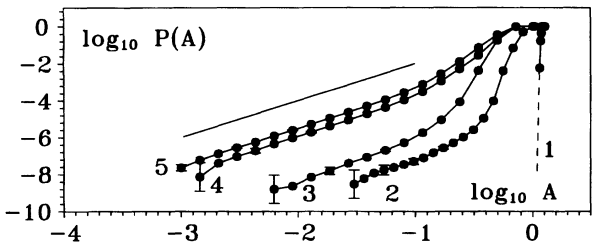

(b)

FIG. 4. (a) Histogram of the amplitude A for $\tau = 0.8$ ms, $B = 160$ V (full circles), and $B = 200$ V (open circles); (b) same as in (a) for Eq. (3) with $\mu = 1$ and $\tau = 50$. Curves 1 to 5 correspond to $\beta = 1.7$, 1.8, 1.9, 2.5, and 3.2. The two straight lines correspond to $P(A) = \text{const}\, A^2$.

a time delayed coupling instead of a spatial coupling. As a further difference, it depends on three control parameters, whereas the CGL is specified by only two. A detailed investigation of the parameter space will be given elsewhere; here we consider the case $\varepsilon = 0$.

A phenomenological analysis of Eq. (3) reveals strong analogies with the experiment. The evidence of phase defects is shown in Fig. 2(c). Defectlike structures are seen to interrupt an otherwise periodic pattern in Fig. 2(d). At variance with the experiment, the amplitude A is directly accessible in the numerical simulations of the model; thus, we can accurately trace the probability distribution $P(A)$. The simulations performed for $\mu = 1$ and $\tau = 50$ [Fig. 4(b)] reveal two distinct regimes. For $\beta < 1.8$, the oscillation amplitude is bounded above a finite value, while for $\beta > 1.9$, the amplitude can be arbitrarily small. Moreover, in the latter regime the various curves are asymptotically parallel to one another. Under the proviso that a true defect can always be found by extending $x(\sigma, n)$ to noninteger n values, the above result can be interpreted as an indication that the 2D defect profile is almost independent of the parameter values. The different heights of the various curves are a measure of the density of defects, which approaches 0 when β is decreased below a critical value. The power-law dependence of the small amplitude probability, with an exponent $\nu = 2$, is in reasonable agreement with the experiment.

The small-A behavior of $P(A)$ permits us to assign the 2D profile $A \simeq r^{\gamma}$ of the amplitude close to a defect (r being the distance from the core), provided the defects are isotropic and randomly positioned with respect to the integer lattice. Indeed, assume a low density of uniformly distributed defects, with mean separation L, and call r the radius where the amplitude has recovered an assigned value A. Let us consider a straight line on the plane. A defect, the core of which is separated by a distance d from that line, provides an amplitude below A over a segment of the line of length $l = \sqrt{r^2 - d^2}$. Averaging over all d, the segment fraction l/L covered by amplitudes below A scales as r^2. Thus, the probability $P(A)$ is given by l/L and it scales as $r^2 = A^{2/\gamma}$. Comparison with the above results yields $\gamma = 1$. Releasing the isotropy assumption does not change this scaling behavior.

In conclusion, we have shown the presence of phase defects in delayed dynamical systems in the limit of long delays. As a consequence, it was possible to distinguish two dynamical regimes. This scenario resembles that reported for 1D SES [11]. However, an exhaustive characterization of such regimes is definitely more accessible in a delayed system; indeed, from the numerical point of view, the discreteness of the "time" variable n allows faster simulations of DDS's, and from the experimental point of view, control of the system size is easily achieved by changing τ, thus permitting an accurate investigation of the scaling properties.

We warmly acknowledge Pasquale Poggi who designed and realized the delay line. This work has been partially supported by EEC–Esprit Basic Research action TONICS (Contract No. 7118).

[1] M. C. Mackey and L. Glass, Science **197**, 287 (1977).
[2] K. Ikeda, Opt. Commun. **30**, 257 (1979).
[3] F. T. Arecchi, G. Giacomelli, A. Lapucci, and R. Meucci, Phys. Rev. A **45**, 4225 (1992).
[4] J. D. Farmer, Physica (Amsterdam) **4D**, 366 (1982).
[5] K. Ikeda and M. Matsumoto, J. Stat. Phys. **44**, 955 (1986).
[6] M. Le Berre, E. Ressayre, A. Tallet, H. M. Gibbs, D. L. Kaplan, and M. R. Rose Phys. Rev. A **35**, 4020 (1987).
[7] B. Dorizzi, B. Grammaticos, M. Le Berre, Y. Pomeau, E. Ressayre, and A. Tallet, Phys. Rev. A **35**, 328 (1987).
[8] S. Lepri, G. Giacomelli, A. Politi, and F. T. Arecchi, Physica (Amsterdam) **70D**, 235 (1994).
[9] F. T. Arecchi, G. Giacomelli, A. Lapucci, and R. Meucci, Phys. Rev. A **43**, 4997 (1991).
[10] M. C. Cross and P. C. Hohenberg, Rev. Mod. Phys. **65**, 851 (1993).
[11] B. J. Shraiman, A. Pumir, W. van Saarloos, P. C. Hohenberg, H. Chaté, and M. Holen, Physica (Amsterdam) **57D**, 241 (1992).
[12] H. Chaté, "Disordered regimes of the one-dimensional complex Ginzburg-Landau equation" (to be published).

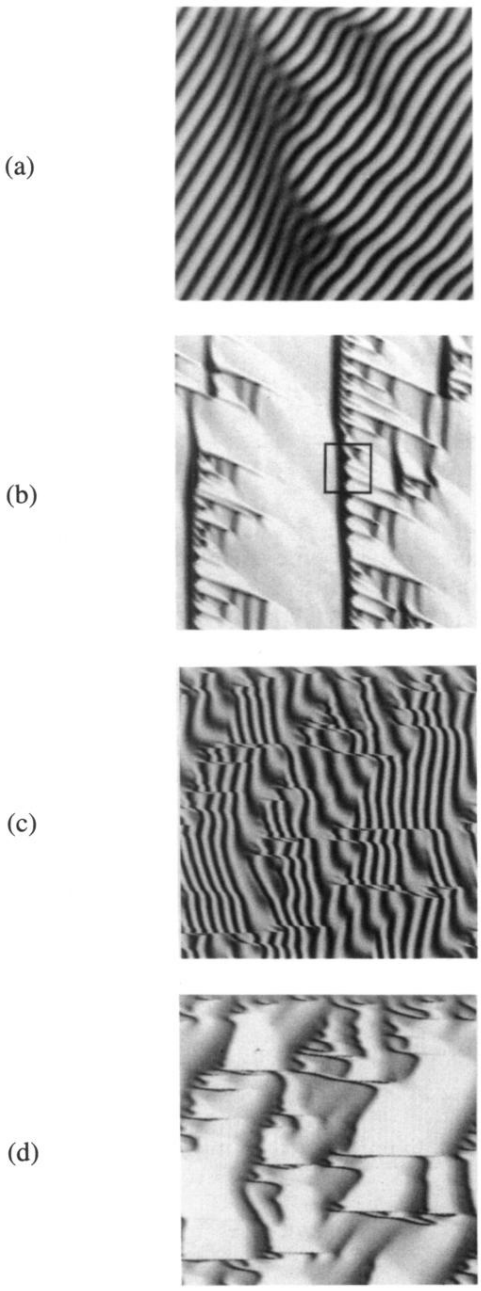

FIG. 2. Space (horizontal)-time (vertical) plots of the experimental signal for $B = 160$ V and $\tau = 0.8$ ms [(a), (b) and of the solutions of (3)] for $\mu = 0.5$, $\beta = 2$, and $\tau = 50$ [(c), (d)]. Time increases downward. (a) is a plot of the actual experimental signal, while (b) is the envelope amplitude after demodulation of the carrier (800 delay units are reported). The pattern in (a) corresponds to the boxed region in (b). The pattern reported in (c) is the 2D representation of $\mathrm{Re}\{x(t)e^{i\omega n}\}$, where $\omega = 1.2$ is a phase shift introduced to better reveal the oscillations of the signal (500 delay units are reported). The corresponding envelope amplitude is shown in (d). In cases (b) to (d), the horizontal width has been suitably set to a value slightly larger than τ to eliminate the systematic drift of the main structures. The defects appear as fringe dislocations in a quasisinusoidal pattern [(a), (c)] or as black regions in the envelope representation [(b), (d)].